Drone Height Estimation from 5G Signals

Enrique Caballero, Aymen Fakhreddine, and Christian Bettstetter
Institute of Networked and Embedded Systems, University of Klagenfurt, Klagenfurt, Austria
E-Mail: enrique.caballero@aau.at

This is the authors' submitted manuscript that has been accepted for presentation at the European Wireless Conference, Rimini, Italy, June 2026. The final published version will be available at the IEEE Digital Library.

***Abstract*—This paper presents a drone height estimation technique based on 5G signal strength to support aerial operations. The approach exploits height-dependent variations of the received power caused by base station antenna patterns and line-of-sight links. By extending a system-level simulator with aerial user and channel models, we generate signal strength data to train machine learning models. Among the evaluated models, an ensemble decision tree achieves the best performance, with a root mean square error below two meters. In different simulated flight scenarios, the estimation error is below 2.5 meters during 95 % of the time. Although the method does not outperform GNSS, it illustrates that cellular connectivity of drones can provide a complementary source of height information.**

***Index Terms*—UAV, 5G, height estimation, RSRP, ML, PNT**

I. Introduction

Positioning, navigation, and timing (PNT) are fundamental functions for drone operations and are typically provided by Global Navigation Satellite Systems (GNSS). However, GNSS signals are vulnerable to blockage, jamming, and spoofing; and many countries depend on foreign satellites, raising concerns about technological sovereignty and resilience. Consequently, GNSS represents a potential point of failure for aerial operations. To ensure resilient drone operation, complementary positioning solutions are required to maintain navigation capabilities during periods of GNSS degradation or denial.

There are several non-GNSS PNT techniques, including radio, magnetic, acoustic, and ultrasonic-based systems [1]. Radio-based techniques are well-investigated, using approaches like time difference, angle of arrival, and received signal strength. Researchers use round-trip timing [2], signals of opportunity [3], and RF fingerprinting and reconfigurable intelligent surfaces [4], [5]. A critical limitation still persists: most techniques are designed primarily for *ground* users, yielding mainly two-dimensional positioning. With the deployment of drones, such planar localization becomes insufficient and calls for **height estimation** techniques to consider the vertical dimension. Height estimation enables safer integration of aerial devices into non-segregated airspace. It is useful for a wide range of tasks, including autonomous navigation, high-precision georeferencing for mapping, surveying, as well as real-time localization for beyond visual line-of-sight operations [6] and safety protocols like return-to-home.

Existing solutions for height estimation use dedicated onboard sensors like barometric pressure sensors, LiDAR, or radar altimeters. Barometers are inexpensive and provide accurate relative altitude measurements but suffer from drift and air pressure variations. LiDAR and radar altimeters provide precise distance measurements to the ground but increase system cost and weight. In contrast, our approach assumes that drones are equipped with a wireless transceiver that connects them to a cellular network. The technique exploits radio signals received from base stations and interprets the reference signal received power (RSRP) using a machine learning model. RSRP is the average power received from a base station and is commonly used for cell selection, handover decisions, and coverage optimization. Our technique analyzes the characteristics of RSRP to infer height, achieving meter-level accuracy in the evaluated scenarios. It can thus provide redundancy to GNSS, enhancing the resilience and integrity of drone missions. The approach could also be used by network operators to detect and classify drones and other aerial users based on their altitude to support network management.

The contributions can be summarized as follows:

- A simulation framework for analyzing drone height estimation using 5G signals and real base station positions
- A machine-learning-based approach that exploits RSRP data from multiple base stations to estimate drone height
- An evaluation of several regression models for height estimation using simulated drone flight data
- Simulation results showing that meter-level height estimation can be achieved in the evaluated scenarios, where the error is below 2.5 m during 95 % of the time

This paper is organized as follows: Section II addresses related work. Section III characterizes the physical propagation environment of cellular-connected drones. Section IV describes the system model and simulation environment. Section V presents the methodology, addressing data acquisition, training of the learning model, and refinement of the estimation via a filter. Section VI presents a performance analysis and compares it against GNSS. Finally, Section VII concludes.

II. Related Work

Our work exploits environmental signals that were not originally intended for positioning [7]–[10]. These "signals of opportunity" serve as a means to achieve assured PNT. Obtaining the distance to aerial vehicles using radio signals has been explored via different methods. Some exploit the time difference of arrival, where achievable bounds are known [11]. The vertical error of using downlink positioning reference signals was identified as one of the main drawbacks, obtaining vertical errors between 10 and 60 m in median, and between 40 and 160 m in worst-case scenarios [12]. Other methods, such as ours, rely on data-driven approaches. Drone positioning can be formulated as an optimization problem using received signal strength indicator measurements from base stations [13],

but typically there is no distinction between vertical and horizontal errors. Some work took a hybrid approach but focused on planar positioning [14]. These results indicate that accurate height estimation remains an open challenge. Building on our work on drone classification [15], we aim to fill this gap by developing a data-driven height estimation algorithm, whose errors remain within reasonable bounds, serving as a complement to GNSS-based solutions.

III. Radio Link Phenomena for Drones

The radio links between aerial drones and base stations differ significantly from those experienced by ground users. Two aspects are particularly relevant in this work: the connection of drones via antenna sidelobes and the presence of line-of-sight links to multiple base stations at elevated heights. These height-dependent link variations create distinctive RSRP patterns that can be exploited by machine learning for the purpose of height estimation.

A. Drones are Connected via Base Station Sidelobes

The primary objective of most cellular deployments is to maximize coverage and performance for ground users while minimizing interference. The antennas of the base stations use mechanical or electrical downtilt or beamforming to direct the main lobe of the radiation pattern toward the ground. When a drone ascends from the ground to a certain height, it leaves the main lobe and moves into sidelobe and void regions of the pattern, suffering from degraded link quality [16]–[18].

An example antenna pattern is shown in Figure 1. The main lobe dominates at low heights near the ground level, resulting in strong and stable RSRP values. An ascending drone leaves the main lobe and enters the lowest sidelobe. At higher heights, the ascending drone experiences a changing pattern consisting of upper sidelobes and voids. At these heights, a vertical displacement of merely a few meters can result in a signal variation of 15–20 dB as the drone moves from a local peak to a void. This non-monotonicity is one of the main artefacts we exploit to develop a machine learning model.

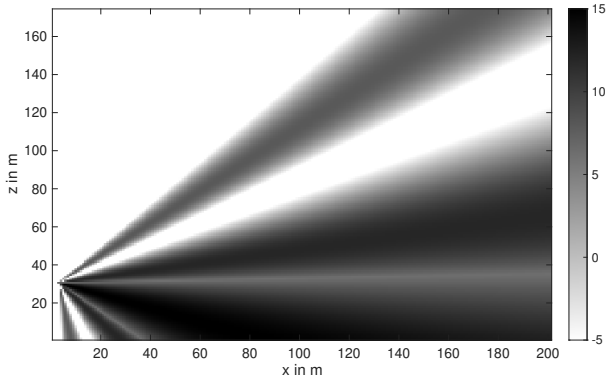

Fig. 1: Antenna: Vertical cut of the gain pattern (in dB) used for the data acquisition based on [19]

B. Drones have Line-of-Sight Links to Multiple Base Stations

The 3GPP standard TR 36.777 [20] defines air-to-ground channel models for aerial vehicles, in which a key parameter is the height-dependent line-of-sight (LoS) probability. This probability approaches 100 % once a drone reaches a certain height. While such strong LoS links were initially considered beneficial, they also lead to strong inter-cell interference [21]–[23]: A high-flying drone has LoS to several distant base stations, which transmit on the same time-frequency channels. As a consequence, the drone receives strong signals from interfering cells, degrading the signal-to-interference-plus-noise ratio (SINR). Although the regression target here is RSRP (signal power), the presence of high interference affects the detection threshold of neighboring cells, altering the composition of the feature vector used for training.

IV. System Model and Simulation Environment

A. Simulator

The Vienna 5G System Level Simulator, which is part of the Vienna Cellular Communications Simulators (VCCS) developed by TU Wien [24], is employed for network simulation. Some modifications and extensions are made to account for the specifics of aerial users. These changes are similar to those in our previous papers [6], [15], [25].

B. Simulated Environment: Buildings, Users, Base Stations

The simulation is conducted for a suburban region of size $1\,\mathrm{km}^2$ around the University of Klagenfurt, Austria (see Figure 2). Buildings are generated using footprints from OpenStreetMap, with heights randomly assigned between 10 and 25 m. Within the simulated region, 400 user equipments (UEs) are deployed per simulation run. Half of the UEs are ground users with heights uniformly distributed between 0 and 30 m. The remaining half are aerial UEs, evenly split into low-altitude aerial users (30–100 m) and high-altitude aerial users (100–250 m). All UEs are randomly distributed, where ground users are placed only outside buildings. The real-world locations of the base stations are taken from the database *Senderkataster* [26]. Antennas are located at a height of 30 m above ground; antennas mounted on buildings are handled in the same way as those on masts.

C. Path Loss Model

The default path loss model in the simulator is meant for users at heights below 22.5 m [19]. To accommodate aerial UEs, we implement an extension following 3GPP recommendations, covering both line of sight (LoS) and non-line of sight (non-LoS) conditions [20]:

$$\mathrm{PL}_{\text{LoS}} = 28 + 22\log d + 20\log f_c$$

$$\mathrm{PL}_{\text{non-LoS}} = (46 - 7\log z)\log d + 20\log\frac{40\pi f_c}{3} - 17.5\,,$$

with distance d between drone and base station in meters, carrier frequency f_c in GHz, and flight height z above ground in meters. Both equations are valid for $22.5\ \mathrm{m} \leq z \leq 300\ \mathrm{m}$.

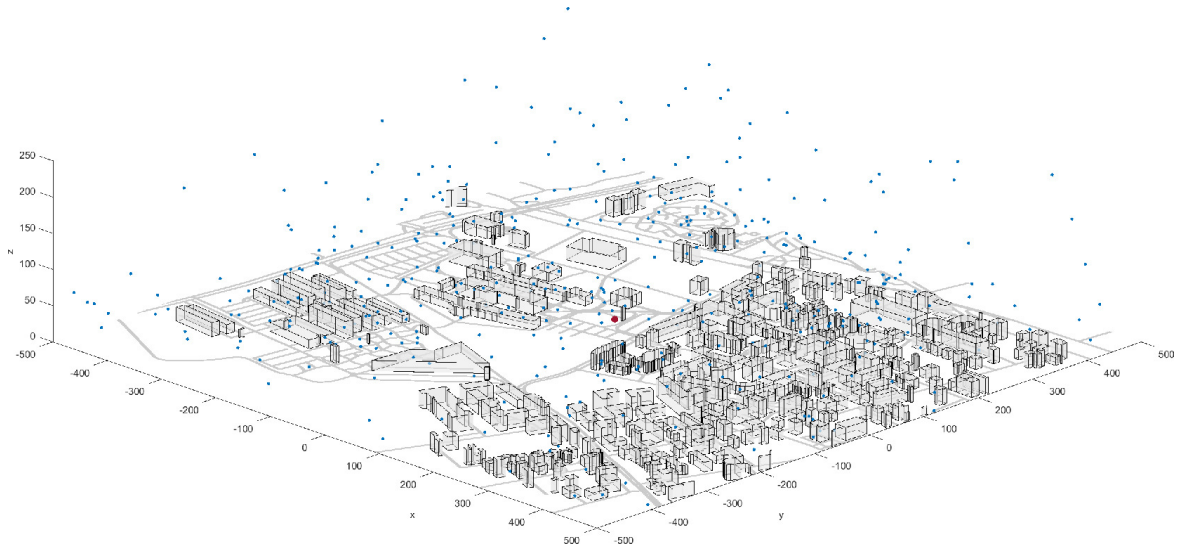

Fig. 2: Snapshot of the simulated area with buildings, base stations, ground devices, and aerial devices

D. Base Station Antennas

The base stations employ a three-sector antenna. The radiation pattern is modeled using analytical expressions derived from 3GPP specifications [19], given in Table I.

TABLE I: Radiation Power Pattern as per [19]

Pattern type	**Expression**
Vertical cut	$A''_{\text{dB}}(\theta'', \phi'' = 0^\circ) = -\min\left\{12\left(\frac{\theta''-90^\circ}{\theta_{\text{3dB}}}\right)^2, \text{SLA}_V\right\}$
Horizontal cut	$A''_{\text{dB}}(\theta = 90^\circ{}'', \phi'') = -\min\left\{12\left(\frac{\phi''}{\phi_{\text{3dB}}}\right)^2, A_{\max}\right\}$
3D pattern	$A''_{\text{dB}}(\theta'', \phi'') = -\min\Big\{-(A''_{\text{dB}}(\theta''=90^\circ, \phi''=0^\circ) + A''_{\text{dB}}(\theta''=90^\circ, \phi'')), A_{\max}\Big\}$
Parameters	$\theta_{\text{3dB}} = 65^\circ$, $\text{SLA}_V = 30$ dB, $\theta'' \in [0^\circ, 180^\circ]$ $\phi_{\text{3dB}} = 65^\circ$, $A_{\max} = 30$ dB, $\phi'' \in [-180^\circ, 180^\circ]$

We adapt the model to simulate a main lobe and two sidelobes. To implement the sidelobes, the standard expressions are modified. The half-power beamwidth, θ_{3dB} and ϕ_{3dB} are scaled to reduce the size relative to the main beam. θ and ϕ are shifted to define the sidelobe orientation relative to the main lobe. The total gain A''_{dB} is reduced by a sidelobe level to decrease the intensity relative to the main lobe. The main lobe is configured with an elevation of 20 degrees (downtilt), with θ_{3dB} and ϕ_{3dB} set to 25 degrees. To simulate the shadow effect behind base stations, the maximum attenuation is set to -90 dB. The two sidelobes are located above the main lobe at relative elevation offsets of -35 and -70 degrees. For these sidelobes, the 3 dB angles are scaled by factors of 0.5 and 0.3, and their gain levels are attenuated by 5 and 7 dB, respectively.

Using the default setting of maximum attenuation being -20 dB, a UE directly behind an antenna still received a very strong signal. This was fixed by changing it to -90 dB, which at least pushes the antennas facing away from the UE below the -120 dBm threshold. These settings are used to obtain RSRP values that are similar to those from our real-world measurement campaign carried out in the same area [27].

E. Simulation Parameters

The system-level simulation parameters are given in Table II. They are similar to our previous papers [15], [25] and match empirical data from our measurements [27].

TABLE II: System-level Parameters

Parameter	**Value**
Frequency	2 GHz
Bandwidth	20 MHz
Number of resource blocks	50
Transmission time interval (TTI)	1 ms
Pathloss	UMa TR36777 [20]
Geometry	Campus Univ. Klagenfurt
Area	1.5 km^2
Number of users	400
User transmission power	23 dBm
Number of antenna elements	16 (4×4)
Base station transmission power	40 dBm
Ground user positions	Random uniform distribution

V. Height Estimation Algorithm

The proposed height estimation approach is illustrated in Figure 3. The process consists of two phases: training and deployment. During the training phase, a simulation scenario is used to generate a large set of RSRP values, from which a height estimation model is derived. In the deployment phase, this model provides an initial estimate $\hat{z}^*$ of the drone height z. This estimate is subsequently refined using a Kalman filter to obtain the final height estimate $\hat{z}$.

A. Machine Learning Model

We simulate a 5G-connected drone that follows a predefined flight path and records RSRP values from the serving cell and

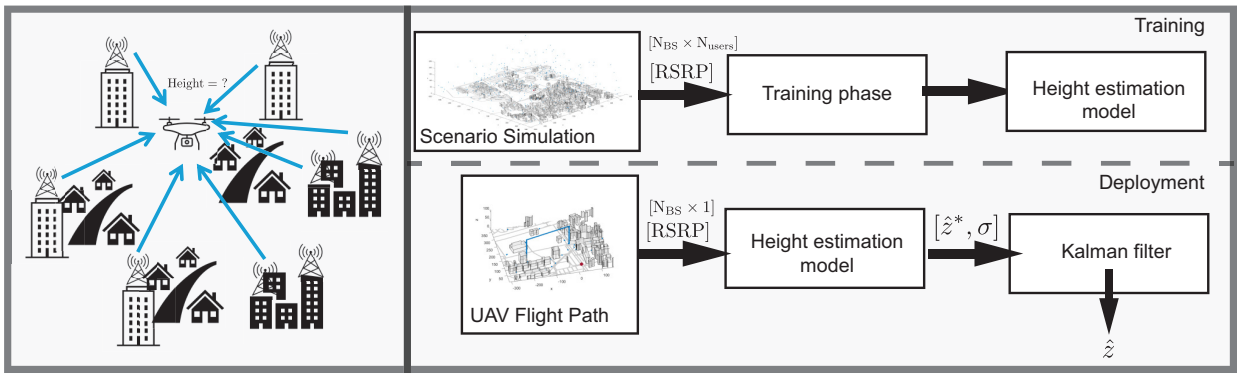

Fig. 3: System model for the estimation workflow, fragmented into the training of the model and its intended deployment

all detectable neighboring cells during its flight. This generates a height-labeled dataset with 6.4 million RSRP samples from 40 three-sector cells with 53,410 values per sector. With MATLAB's Statistics and Machine Learning Toolbox, we partition the data into training and validation sets (80 %/20 %). A cross-validation framework is used to benchmark several regressors, including trained k-nearest neighbors, linear regressions, single decision trees, support vector machines, ensemble tree methods, and neural networks.

To assess generalization and prevent overfitting, we evaluate the models against an independent test set. It consists of the previous simulation scenario with the same number of users and characteristics, but recording a drone's RSRP over different flight paths. The estimation is assessed using the root mean square error (RMSE) between predicted and actual heights.

B. Navigation Model

To evaluate whether the trained model is suitable for drone navigation, we compare its inference with simple GNSS sensor measurements. For that purpose, we use a navigation model: a state-space representation of how the drone moves over time. The navigation architecture incorporates the trained machine learning model to refine the measurement. At each time step, as the drone traverses the 5G coverage area, the height estimation model trained on the data processes the instantaneous vector of RSRP values to generate a raw height prediction. This prediction is paired with the corresponding RMSE. This RMSE serves as a quantifier of the observation noise, informing the system of how much trust to place in the radio-based height reading. Let us outline the model used to validate the navigation enhancement based on radio-based height readings. The full approach is given in Algorithm 1.

The vertical dynamics of the drone is modeled using a simple discrete-time linear state-space representation. The state vector $\mathbf{x}_k$ at time step k consists of height and vertical velocity and evolves with step size Δt according to the state transition equation $\mathbf{x}_k = \mathbf{A}\,\mathbf{x}_{k-1}$ with state transition matrix

$$\mathbf{A} = \begin{bmatrix} 1 & \Delta t \\ 0 & 1 \end{bmatrix}.$$

Algorithm 1: Drone Sensor Fusion: ML Estimation and Kalman Filtering

Data: Simulation Scenario $\mathcal{S}$, ML Models $\mathcal{M}$, System Matrices $\mathbf{A}, \mathbf{H}, \mathbf{Q}, \mathbf{R}$
Result: Estimated Height $\hat{z}$

/* **GNSS data and Height Inference** */
Initialize dataset $\mathcal{D} \leftarrow \emptyset$
while *Simulation is Running* **do**
  Step simulation $\mathcal{S}$
  Acquire noisy GNSS measurement $\mathbf{z}_{gnss}$
  Acquire RSRP signals. Predict height $\hat{z}_{ml}$ using $\mathcal{M}$
  $\mathbf{z}_k \leftarrow \{\hat{z}^*_{gnss}, \hat{z}^*_{ml}\}$
  Append $\mathbf{z}_k$ to $\mathcal{D}$
end
/* **State Estimation** */
Initialize state estimate $\hat{\mathbf{x}}_0$ and covariance $\mathbf{P}_0$
for $k \leftarrow 1$ **to** T **do**
  /* Prediction Phase */
  $\hat{\mathbf{x}}_k^- \leftarrow \mathbf{A}\hat{\mathbf{x}}_{k-1}$
  $\mathbf{P}_k^- \leftarrow \mathbf{A}\mathbf{P}_{k-1}\mathbf{A}^\top$
  /* Correction Phase */
  Retrieve measurement $\mathbf{z}_k$ from $\mathcal{D}$ (GNSS or ML-Height)
  Compute Kalman Gain: $\mathbf{K}_k \leftarrow \mathbf{P}_k^-\mathbf{H}^\top(\mathbf{H}\mathbf{P}_k^-\mathbf{H}^\top + \mathbf{R})^{-1}$ with $\mathbf{H} = [1\ 0]$
  Update State: $\hat{\mathbf{x}}_k \leftarrow \hat{\mathbf{x}}_k^- + \mathbf{K}_k(\mathbf{z}_k - \mathbf{H}\hat{\mathbf{x}}_k^-)$
  Update Covariance: $\mathbf{P}_k \leftarrow (\mathbf{I} - \mathbf{K}_k\mathbf{H})\mathbf{P}_k^-$
end
return Filtered State $\hat{\mathbf{X}} = \{\hat{\mathbf{x}}_1, \ldots, \hat{\mathbf{x}}_T\}$

Prediction phase: This system model is used to predict the state and error covariance matrix (lines 11 and 12 in Algorithm 1), where these predictions are denoted as $\hat{\mathbf{x}}_k^-$ and $\mathbf{P}_k^-$, respectively. The process noise is assumed to be negligible. The error covariance matrix is initialized by

$$\mathbf{P}_0 = \begin{bmatrix} 0.5 & 0 \\ 0 & 0.7 \end{bmatrix}.$$

Correction phase: The Kalman gain $\mathbf{K}_k$ is computed from the prediction error covariance matrix $\mathbf{P}_k^-$, measurement matrix $\mathbf{H}$, and measurement error covariance matrix $\mathbf{R}$. The latter depends on the technology used and is $R = \sigma^2_{\text{GNSS}} = 2.25\ \text{m}^2$ for GNSS. The navigation model observes the height estimate from the trained model's output or from the GNSS sensor. This measurement is used to update both state and covariance (lines 15 and 16 in Algorithm 1).

Output: After all iterations, a series of state estimates $\hat{\mathbf{x}}_1, \ldots, \hat{\mathbf{x}}_T$ results, each value containing a height estimation $\hat{z}_k$.

VI. Performance Evaluation

A. Choice of Learning Algorithm

To identify a machine learning (ML) algorithm suitable for height estimation, we test several standard algorithms and compare their performance. Two flight types are used: a vertical ascent from the ground to 250 m and a series of cruise flights at different heights (including ascent and descent).

Figure 4 shows the results for the vertical ascent, comparing the height inference of an ensemble decision tree, a generalized linear regression, and a generalized additive model. The ensemble decision tree captures the flight path with a reasonable RMSE of 1.6 m. The linear regression model does not perform well across the entire flight path, with an RMSE of 72.5 m, mainly due to the non-linear nature of the received signal. The additive model performs comparably to the ensemble decision tree most of the time but does not capture the abrupt pathloss change when the drone crosses the height of buildings at 25 meters, leading to an RMSE of 5.5 m. Other algorithms like k-nearest neighbors, fully-connected neural network, and support vector machine were tested as well but performed poorly. Hence, our choice is to use the ensemble decision tree as our learning model.

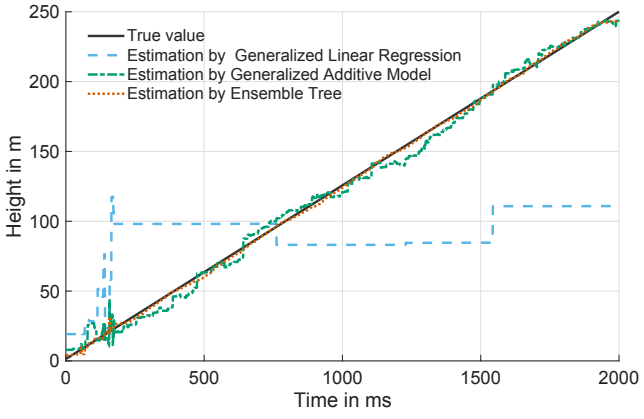

Fig. 4: Height estimation for an ascending drone using three algorithms: ensemble decision tree, generalized linear regression, and generalized additive model

To verify this choice, Figure 5 shows the performance of the ensemble decision tree for cruise flights at 40, 80, and 100 m. The inferred RMSE remains between 1.0 and 1.3 m, which is a good starting point for navigation, fulfilling positioning requirements in the order of several decimeters.

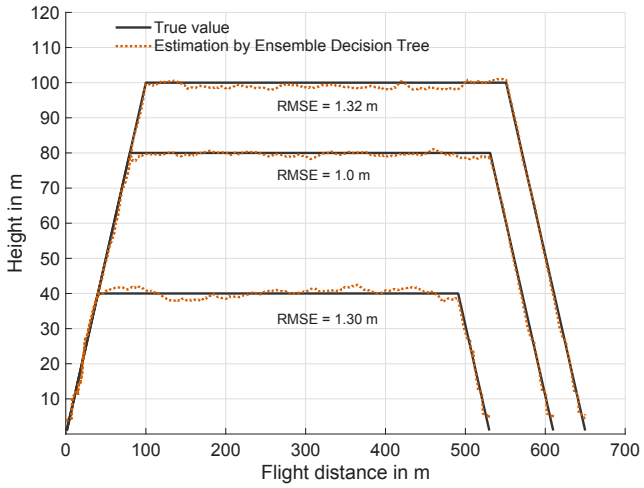

Fig. 5: Height estimation for a drone performing cruise flights at three different heights using ensemble decision tree

B. Performance Comparison with GNSS

The height estimation technique based on an ensemble decision tree is now further evaluated and compared with GNSS-based estimation. Two scenarios are simulated: (a) a drone performing a vertical ascent over 20 s and (b) a drone ascending to 80 m, performing a cruise flight at this height, and descending again, with a duration of 200 s. The GNSS sensor is implemented in MATLAB using the Navigation Toolbox.

Figure 6 shows the estimation errors over time: the raw estimation error at a given time (blue curve) and the Kalman filter-smoothed error (red curve) for both RSRP-based inference (top plots) and GNSS (bottom plots). The filter smooths the temporal dynamics and reduces errors that occur when the drone transitions above building heights. The ascent and landing phases exhibit a higher error variance than the cruise phase.

TABLE III: Height estimation error (values in meters).

Scenario	Method	Error			
		Median	RMSE	95 %	99 %
(a) Ascent	RSRP-based	1.18	1.45	2.44	3.12
	GNSS	0.40	0.56	1.19	1.67
(b) Cruise	RSRP-based	0.25	0.94	2.01	2.93
	GNSS	0.34	0.75	1.89	1.97

The overall error statistics are given in Table III and Figure 7. For the ascending drone, the median error is 1.18 m (RSRP) and 0.4 m (GNSS), and 95 % of all estimates have an error below 2.44 m (RSRP) and 1.19 m (GNSS). For the cruise flight, both median errors are an order of magnitude lower, namely 0.17 m (RSRP) and 0.25 m (GNSS), and the 95 % error quantiles now are very similar, namely 2.01 m (RSRP) and 1.89 m (GNSS). This behavior is also visible in the empirical complementary cumulative distribution function

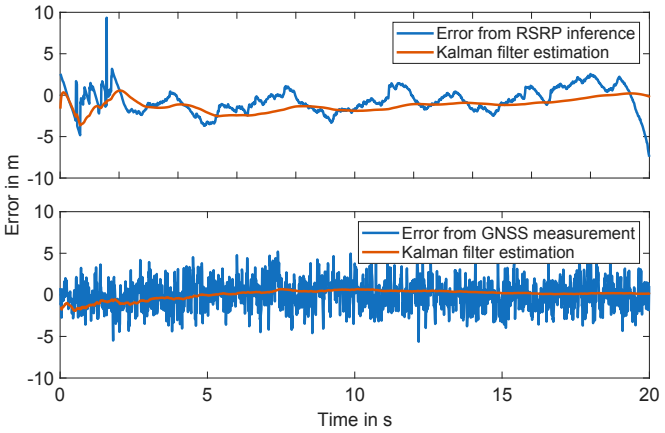

(a) Drone ascending from the ground to 250 m

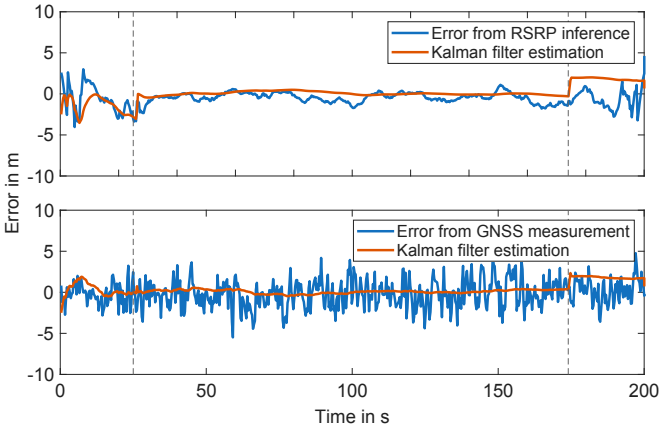

(b) Drone on a cruise flight at 80 m

Fig. 6: Height estimation error using RSRP data and GNSS. Raw estimation errors (blue curves) and Kalman filter-smoothed estimation errors (red curves)

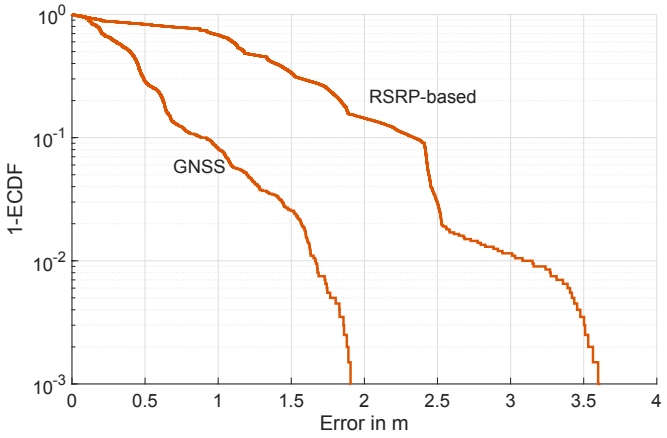

(a) Drone ascending from the ground to 250 m

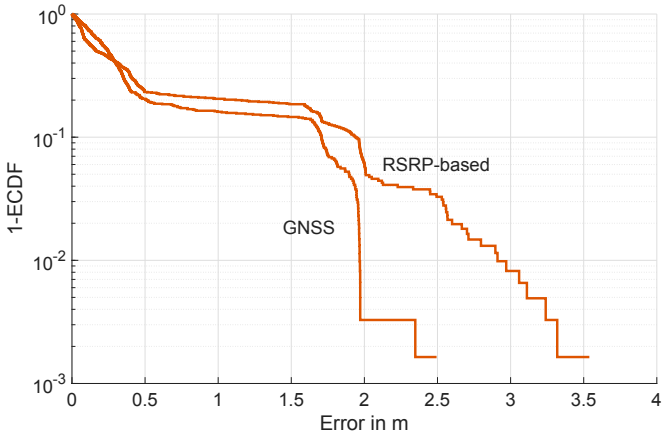

(b) Drone on a cruise flight at 80 m

Fig. 7: Empirical complementary cumulative distribution function (ECCDF) of the height estimation error using RSRP data and GNSS with Kalman filter correction

(ECCDF) of the height estimation error given in Figure 7. Each ECCDF curve shows the fraction of height estimates whose error exceeds the value shown on the horizontal axis.

In summary, although the use of GNSS for height estimation remains superior, the RSRP-based technique performs relatively well and its errors remain within acceptable bounds.

VII. Conclusions and Outlook

This paper proposed and evaluated a learning-based height estimation technique for drones using signals from cellular networks. Results based on simulated RSRP data indicate that an estimation accuracy of between one and two meters can be achieved. The approach can complement GNSS-based solutions and enhance the resilience of height estimation in GNSS-challenged environments [2].

The next steps include validating the approach in field experiments using drones in a real 5G network and analyzing its sensitivity to environmental conditions and antenna patterns.

Acknowledgments

This work has been funded by the Austrian Science Fund (FWF – Der Wissenschaftsfonds) under grant ESPRIT-54 (Grant DOI: 10.55776/ESP54). The authors used Grammarly, ChatGPT, Gemini, and DeepL for language improvements.

References

[1] F. Lateef, M. Kas, and Y. Ruichek, "From GPS to AI: A comprehensive review of unmanned aerial vehicle (UAV) localization solutions," *ISPRS J. of Photogrammetry and Remote Sensing*, vol. 230, pp. 402–451, 2025.

[2] F. Campolo, A. Blaga, M. Rea, A. Lozano, and X. Costa-Pérez, "5GNSS: Fusion of 5G-NR and GNSS localization for enhanced positioning accuracy and reliability," *IEEE Trans. on Vehicular Technology*, 2024.

[3] J. Khalife and Z. M. Kassas, "Navigation with cellular CDMA signals of opportunity," *IEEE Trans. on Aerospace and Electronic Systems*, 2018.

[4] M. Ezuma, F. Erden, C. K. Anjinappa, O. Ozdemir, and I. Guvenc, "Detection and classification of UAVs using RF fingerprints in the presence of Wi-Fi and Bluetooth interference," *IEEE Open Journal of the Communications Society*, 2020.

[5] D. Dardari, "Communicating with smart radio environments: The role of intelligent surfaces in localization," *IEEE Signal Processing Magazine*, 2021.

[6] E. Caballero, C. Bettstetter, D. Schupke, and A. Fakhreddine, "Command and control of drones over 5G," in *Proc. IEEE INFOCOM Workshop on Networked Robotics and Communication Systems*, Tokyo, Japan, Jun. 2026.

[7] W. Stock, R. T. Schwarz, C. A. Hofmann, and A. Knopp, "Survey on opportunistic PNT with signals from LEO communication satellites," *IEEE Communications Surveys & Tutorials*, 2025.

[8] F. S. Prol, R. M. Ferre, Z. Saleem, P. Välisuo, C. Pinell, E. S. Lohan, M. Elsanhoury, M. Elmusrati, S. Islam, K. Çelikbilek, K. Selvan, J. Yliaho, K. Rutledge, A. Ojala, L. Ferranti, J. Praks, M. Z. H. Bhuiyan, S. Kaasalainen, and H. Kuusniemi, "Position, navigation, and timing (PNT) through low earth orbit (LEO) satellites: A survey on current status, challenges, and opportunities," *IEEE Access*, 2022.

[9] K. Shamaei, J. Khalife, and Z. M. Kassas, "Exploiting LTE signals for navigation: Theory to implementation," *IEEE Trans. on Wireless Communications*, 2018.

[10] Z. Z. M. Kassas, J. Khalife, K. Shamaei, and J. Morales, "I hear, therefore I know where I am: Compensating for GNSS limitations with cellular signals," *IEEE Signal Processing Magazine*, 2017.

[11] C. Dickerson, S. Masrur, J. Dickerson, O. Ozdemir, and I. Guvenç, "Impact of altitude, bandwidth, and NLOS bias on TDOA-based 3D UAV localization: Experimental results and CRLB analysis," in *Proc. IEEE Intern. Conf. on Communications (ICC) Workshops*, 2025.

[12] X. Wang, Y. Zhang, Y. Li, and T. Zhang, "5G and UAV integrated three dimensional positioning using downlink PRS," in *Proc. IEEE GLOBECOM*, 2024.

[13] G. Afifi and Y. Gadallah, "Unmanned aerial vehicles 3-D autonomous outdoor localization: A deep learning approach," in *Proc. IEEE Wireless Communications and Networking Conf. (WCNC)*, 2022.

[14] D. A. Maigualema-Quimbita, V. M. Melero, D. Gomez-Barquero, and J. V. B. Tejedor, "Positioning of unmanned aerial vehicles (UAVs) in urban environments using 5G networks: A hybrid approach based on multilateration and machine learning," in *Proc. Integrated Communications, Navigation and Surveillance Conf. (ICNS)*, 2025.

[15] F. Posch, A. Fakhreddine, E. Caballero, and C. Bettstetter, "A classifier for aerial devices in 5G networks," in *Proc. IEEE GLOBECOM Workshop on Cellular UAV and Satellite Communications*, Dec. 2023.

[16] D. Mishra and E. Natalizio, "A survey on cellular-connected UAVs: Design challenges, enabling 5G/B5G innovations, and experimental advancements," *Computer Networks*, vol. 182, p. 107451, 2020.

[17] Z. Cui, K. Guan, I. Güvenç, C. Oestges, and Z. Zhong, "Coverage analysis of cellular-connected UAV communications with 3GPP antenna and channel models," in *Proc. IEEE GLOBECOM*, 2021.

[18] A. Fakhreddine, C. Raffelsberger, M. Sende, and C. Bettstetter, "Experiments on drone-to-drone communication with Wi-Fi, LTE-A, and 5G," in *Proc. IEEE GLOBECOM Workshop on Cellular UAV and Satellite Communications*, Dec. 2022.

[19] 3GPP, "Study on channel model for frequencies from 0.5 to 100 GHz," 3rd Generation Partnership Project (3GPP), Technical Report (TR) 38.901, 2022.

[20] 3GPP, "Study on Enhanced LTE support for aerial vehicles," 3rd Generation Partnership Project (3GPP), Technical Report (TR) 36.777, 2017.

[21] B. Van Der Bergh, A. Chiumento, and S. Pollin, "LTE in the sky: trading off propagation benefits with interference costs for aerial nodes," *IEEE Communications Magazine*, 2016.

[22] E. Vinogradov, H. Sallouha, S. De Bast, M. M. Azari, and S. Pollin, "Tutorial on UAVs: A blue sky view on wireless communication," *Journal of Mobile Multimedia*, 2018.

[23] U. Challita, W. Saad, and C. Bettstetter, "Interference management for cellular-connected UAVs: A deep reinforcement learning approach," *IEEE Trans. on Wireless Communications*, vol. 18, no. 4, pp. 2125–2140, Apr. 2019.

[24] M. K. Müller, F. Ademaj, T. Dittrich, A. Fastenbauer, B. Ramos Elbal, A. Nabavi, L. Nagel, S. Schwarz, and M. Rupp, "Flexible multi-node simulation of cellular mobile communications: The Vienna 5G System Level Simulator," *EURASIP Journal on Wireless Communications and Networking*, vol. 2018, no. 1, p. 227, Dec. 2018.

[25] E. Caballero, A. Fakhreddine, and C. Bettstetter, "Interference by drones to 5G ground users: A simulation study," in *Proc. ACM Workshop on Micro Aerial Vehicle Networks, Systems, and Appl. (DroNet)*, 2023.

[26] Forum Mobilkommunikation, "Senderkataster.at."

[27] A. Fakhreddine, C. Bettstetter, S. Hayat, R. Muzaffar, and D. Emini, "Handover challenges for cellular-connected drones," in *Proc. Workshop on Micro Aerial Vehicle Networks, Systems, and Appl. (DroNet)*, 2019.